# INTERNATIONAL SOCIETY FOR SOIL MECHANICS AND GEOTECHNICAL ENGINEERING



This paper was downloaded from the Online Library of the International Society for Soil Mechanics and Geotechnical Engineering (ISSMGE). The library is available here:

### https://www.issmge.org/publications/online-library

This is an open-access database that archives thousands of papers published under the Auspices of the ISSMGE and maintained by the Innovation and Development Committee of ISSMGE.

The paper was published in the proceedings of the 20<sup>th</sup> International Conference on Soil Mechanics and Geotechnical Engineering and was edited by Mizanur Rahman and Mark Jaksa. The conference was held from May 1<sup>st</sup> to May 5<sup>th</sup> 2022 in Sydney, Australia.

### Use of downscaled SMAP L4 soil moisture data in landslide stability analysis

Utilisation des données d'humidité du sol SMAP L4 à échelle réduite dans l'analyse de stabilité des glissements de terrain

### L. Sebastian Bryson, Daniel Francis & Michelle Imarah

Department of Civil Engineering, University of Kentucky, United States of America, sebastian.bryson@uky.edu

ABSTRACT: This study addresses the feasibility of downscaling SMAP Level 4 Root Zone Soil Moisture and its subsequent use in landslide slope stability analyses. This was conducted by; (1) Acquiring Level 4 soil moisture (L4\_SM) data from the NASA SMAP satellite mission, (2) Downscaling the data from 9 km to 1 km resolution using MODIS and VIIRS 1 km data and the soil moisture and Soil Evaporative Efficiency (SEE) relationship, (3) Locally calibrating the downscaled data to that of ground-based data, and (4) Using the calibrated downscaled data to detect incipient failure conditions within slope stability models created based upon known landslide occurrences. The known landslide events used were the Mud Creek landslide in California USA, The Rattlesnake Hills landslide in Washington USA, and the Sierra Leone landslide near Freetown, Sierra Leone. It was observed that stability models constructed using downscaled L4\_SM data detected strength weakening and incipient conditions well at the investigated sites. The intent of this study is to provide a downscaling and local calibration routine for SMAP L4\_SM data as well as investigating the potential strength of utilizing downscaled L4\_SM data in incipient landslide condition detection.

RÉSUMÉ: Cette étude porte sur la faisabilité de réduire l'humidité du sol de la zone racinaire de niveau 4 SMAP et son utilisation ultérieure dans les analyses de stabilité des pentes de glissement de terrain. Cela a été mené par; (1) Acquisition des données d'humidité du sol de niveau 4 (L4\_SM) de la mission satellite SMAP de la NASA, (2) Réduction d'échelle des données de 9 km à 1 km de résolution en utilisant les données MODIS et VIIRS 1 km et l'humidité du sol et l'efficacité d'évaporation du sol (SEE) relation, (3) étalonner localement les données à échelle réduite à celles des données au sol, et (4) utiliser les données étalonnées à échelle réduite pour détecter les conditions de défaillance naissantes dans les modèles de stabilité des pentes créés sur la base d'occurrences connues de glissements de terrain. Les événements de glissement de terrain connus utilisés étaient le glissement de terrain de Mud Creek en Californie aux États-Unis, le glissement de terrain de Rattlesnake Hills à Washington aux États-Unis et le glissement de terrain en Sierra Leone près de Freetown, en Sierra Leone. Il a été observé que les modèles de stabilité construits à l'aide de données L4\_SM à échelle réduite détectait bien un affaiblissement de la résistance et des conditions naissantes sur les sites étudiés. Le but de cette étude est de fournir une routine de réduction d'échelle et d'étalonnage local pour les données SMAP L4\_SM ainsi que d'étudier la force potentielle de l'utilisation de données L4\_SM à échelle réduite dans la détection de l'état de glissement de terrain naissant.

KEYWORDS: downscaling, satellite, landslides, calibrations, & stability

### 1 INTRODUCTION

Landslides are geological phenomena known to cause significant loss of life and billions of dollars in damages each year (Terzis et al., 2006). The ability to accurately predict, monitor, and provide early warning for where and when a landslide is expected to occur is a resoundingly important task in the attempts to mitigate the damages and losses caused by these slides.

Soil moisture (SM) is a predominant controlling factor of landslide occurrence (Hong et al., 2007). However, acquisition of SM at potential landslide sites can be a tedious and costly endeavor. Fortunately, remote sensing allows for a more readily means of SM acquisition. Due to its sensitivity to subsurface SM and relative insensitivity to vegetation, low-frequency passive microwave remote sensing has been established as the primary tool for retrievals of SM on a global scale. The research data presented in this paper makes use of the Level 4 Root Zone Soil Moisture (L4 SM) product (0-100 cm of the soil column) from the National Aeronautics and Space Administration (NASA) Soil Moisture Active Passive (SMAP) satellite mission. L4 SM is available in a 9 km gridded spatial resolution. While 9 km is not an overly coarse resolution, a finer resolution (e.g., 1 km) is desired for use in applications such as landslide slope stability analysis. Therefore, a means to downscale the L4\_SM product from 9 km to a finer resolution such as 1 km is desired. The research presented herein exploits the assumed relationship between SM and Soil Evaporative Efficiency (SEE) (Merlin et al., 2008) to downscale the L4 SM data. The SEE was calculated using 1 km Land Surface Temperature (LST) and Normalized Difference Vegetation Index (NDVI) data as well as 9 km upscaled LST and NDVI data. After downscaling using the SM/SEE relationship, the downscaled L4\_SM (9 km to 1 km) data was calibrated with ground-based data and then assimilated with easily obtained physical land surface data. The downscaled assimilated data was then used in conjunction with an infinite slope limit equilibrium stability model at known landslide sites to develop site specific stability models. Therefore, this research develops the framework upon which higher resolution remotely sensed SM can be retrieved via downscaling and then utilized for the application of landslide slope stability analysis.

### 2 SATELLITE DATA ACQUISITION

For this study, three parameters were retrieved via remotely sensed data; Root Zone Soil Moisture (L4\_SM), Land Surface Temperature (LST), and Normalized Difference Vegetation Index (NDVI). L4\_SM data were retrieved from the SMAP satellite mission while LST and NDVI were retrieved from the following missions: (1) Moderate Resolution Imaging Spectroradiometer (MODIS) aboard the Aqua and Terra Earth Observing System (EOS). (2) The Visible Infrared Imaging Radiometer Suite (VIIRS) aboard the Suomi National Polar-Orbiting Partnership (NPP) satellite mission.

### 2.1 Satellite-Based L4\_SM Retrievals

Level 4 (SMAP L4\_SM) product is model-derived value-added product obtained by merging SMAP observations with estimates from a Catchment land surface model (LSM) in a data

assimilation system. The model-derived product produces 3-hourly estimates of surface and root zone soil moistures (to a depth of 100 cm) at a 9 km gridded resolution, with a data availability latency of 7 to 14 days (Chan et al., 2016). The SMAP L4\_SM product used for this current study was accessed and acquired using the Application for Extracting and Exploring Analysis Ready Samples (AppEEARS) tool.

### 2.2 Satellite-Based LST and NDVI Retrievals

The L3 daily MODIS Aqua, MODIS Terra, and VIIRS LST and 16-day MODIS Aqua, MODIS Terra, and 8-day VIIRS NDVI product on the 1 km global grid was used in this study. Version 6 of the MODIS products (LST: MOD11A1 and MYD11A1, NDVI: MOD13A2 and MYD13A2) and Version 1 of the VIIRS products (LST: VNP21A1D, NDVI: VNP13A2) were retrieved. The LST and NDVI data were resampled to impute missing daily observations. Once imputed, the 1 km data retrievals were upscaled to a 9 km grid to match the resolution of L4\_SM for use in the SM/SEE relationship. Data imputation and upscaling methods used are discussed fully in following sections. As with L4\_SM data, MODIS and VIIRS data were retrieved using the AppEEARS tool.

### 3 LOCAL CALIBRATION AND LANDSLIDE STUDY SITES

For the downscaling procedures discussed, the data was first downscaled using the SM/SEE relationship. The downscaled data was then locally calibrated to ground-based sensor data. Therefore, the 9 km L4\_SM data was not only downscaled from 9 km to 1 km but was also compared and calibrated to ground-based data. For the stability analyses, three known landslide locations were investigated. The following information was known for each of the three investigated slides: the geographical location of the slide, the failure date of the slide (i.e., when the slide was reported to have occurred), and a relative description of the site after the slide occurred (i.e., damages, type of slide, extent of slide, etc.). These data were used in conjunction with the downscaled and calibrated SMAP L4\_SM and ground surface data to evaluate the hydrologic conditions leading to the incipient failure conditions at each site.

### 3.1 Ground-Based Calibration Sites

This study made use of two sources of ground-based root zone soil moisture data: (1) The Soil Climate Analysis Network (SCAN) maintained by the National Resources Conservation Service (NRCS) and (2) The U.S. Climate Reference Network (USCRN) maintained by the National Oceanic and Atmospheric Administration (NOAA). The name and location of these ground-based data stations is given in Table 1.

Table 1. Ground-Based Sensor Locations

Table 1: Glodina Based Schsol Eccations						
Network	Network Station Name		Longitude			
SCAN	Cook Farm Field	46.78	-117.08			
SCAN	Lind #1	47.00	-118.57			
USCRN	Santa Barbara	34.41	-119.88			
USCRN	Yosemite	37.76	-119.82			

#### 3.2 Investigated Landslides

Three known landslides were investigated during the slope stability analysis phase of this study. The landslides used in this study are as follows: (a) The Mud Creek Landslide, Big Sur, CA, (b) The Rattlesnake Hills Landslide, Union Gap, WA, and (c) The Sierra Leone Landslide near Freetown, Sierra Leone. Table 2 shows the failure date, type of failure, location, as well as which

ground-based station network was used for each slide. As a note, there were no ground-based stations readily available for use with the Sierra Leone landslide. Due to this, no downscaling or calibrations were able to be confidently conducted at this landslide location.

Table 2. Information on Investigated Landslides

Landslide	Date	Latitude	Longitude	Network
Mud Creek	May 20 <sup>th</sup> 2017	35.87	-121.43	USCRN
Rattlesnake Hills	October 2017	46.52	-120.31	SCAN
Sierra Leone	August 14 <sup>th</sup> 2017	8.43	-13.22	N/A

Figure 1 shows the location of each investigated landslide as well as the ground-based stations in relation to the respective slide. The landslides are represented by the "star" symbol while ground-based stations are shown by the circular symbols. As discussed, Sierra Leone had no available ground-based stations, so only the landslide is shown in that instance.

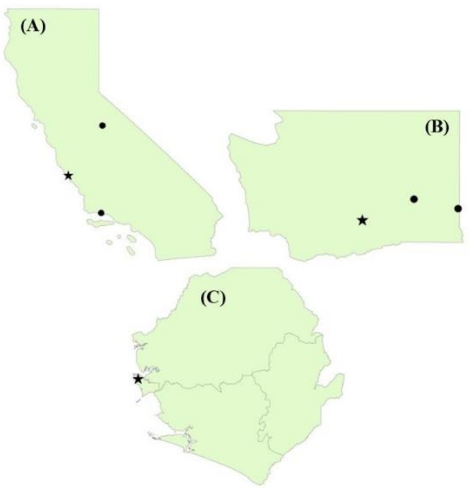


Figure 1. (A) California, USA Landslide & USCRN Locations, (B) Washington, USA Landslide and SCAN Locations, and (C) Freetown, Sierra Leone Landslide Location.

## 4~ DOWNSCALING AND LOCALIZED CALIBRATION OF SMAP L4 $\,$ SM

All the SMAP Level 2, Level 3, and Level 4 products, as well as the Radiometer Level 1C product, employ the Equal-Area Scalable Earth2.0 (EASE2.0) Grid (also referred to as the WGS 1984 Cylindrical Equal Area) projection (Brodzik et al., 2012). Therefore, the L4\_SM data is available in 9 km grids within the EASE2.0 projection. It is crucial to ensure that data retrieved from other satellite platforms (e.g., MODIS and VIIRS) align with these EASE2.0 grids for use in downscaling. The generalized procedure for the downscaling and calibration process is as follows:

### 4.1 Determination of EASE2.0 Grid Center and Extents

The National Snow and Ice Data Center (NSIDC) has created a tool which converts row/column coordinates of EASE2.0 grids (obtained from AppEEARS retrievals in this study) to the latitude and longitude at the center of the grid cell. The program, easeconv.pro, can be either ran in an Interactive Data Language (IDL), C code, or Fortran code and is readily available to the public from the NSIDC (<a href="https://nsidc.org/data/ease/tools">https://nsidc.org/data/ease/tools</a>). For this study, the EASE-Grid data tool easeconv.pro was ran in an IDL environment. To convert from column/row to

latitude/longitude, the following commands were used in the IDL environment:

status=ease\_inverse('EASE2\_M09km',col,row,lat,long) (Command 2)

Command 1 runs the overall program while Command 2 converts from column/row coordinates to latitude/longitude coordinates. In this case, the conversion was being conducted over the global EASE2.0 9 km grids (EASE2\_M09km). However, the program can function with any of the EASE2.0 grids (Northern, Southern, Global, and varying sizes).

To represent the extents of the EASE2.0 9 km grids, ArcGIS was utilized. The projection within ArcGIS was set to be that of WGS 1984 Cylindrical Equal Area. The center of each 9 km grid (found using easeconv.pro) was then input into ArcGIS and was used as the center point of a 9 km square buffer. To ensure the 9 km buffer aligned correctly with the EASE2.0 grid, L4\_SM from the same EASE2.0 grid was retrieved and overlain, with a perfect alignment occurring. Shapefiles of each created buffer were then created and later used to retrieve LST/NDVI data over each of the 9 km grids. Table 3 shows the location that each grid provides data for, the row/column, and latitude longitude coordinates of the center of the grids. It is necessary to note that the location is NOT at the center of the grid. The location simply falls within the 9 km grid.

Table 3. Row/Columns of EASE2.0 Converted to Lat/Lon at Center of Each Grid

Location	Column	Row	Latitude	Longitude
Santa Barbara	643	352	34.435	-119.922
Yosemite	644	314	37.741	-119.829
Mud Creek	627	335	35.897	-121.416
Cook Farm Field	673	219	46.758	-117.121
Lind #1	657	217	46.963	-118.615
Rattlesnake Hills	639	221	46.553	-120.296
Sierra Leone	1786	693	8.397	-13.211

### 4.2 Retrieving LST and NDVI Data

The SM/SEE relationship used for the downscaling routine within this study requires both fine scale and coarse scale SEE (Colliander et al., 2017). Fine scale SEE refers to that of the intended downscaled resolution (i.e., 1 km). For fine SEE, native resolution (1 km) LST/NDVI data was able to be retrieved and averaged across the three platforms (MODIS Aqua, MODIS Terra, and VIIRS). However, it was seen that the daily LST data from all platforms was seen to have large gaps in the time series data. This was likely caused by excessively cloudy days and the fact that cloud cover is a common problem for visible and infrared sensing (i.e., LST sensing). To remedy these large gaps in the data, data imputation was utilized. To impute missing data, the daily LST data was plot as a scatterplot, a 6th order polynomial line of best fit was fit to the data, and the resulting best fit equation was used to fill in missing data. This imputation method was seen to match the pattern of the LST data well.

### 4.3 Upscaling LST and NDVI Data

Coarse SEE, in this case SEE with a spatial resolution of 9 km, implies the need for LST/NDVI data at a resolution of 9 km. However, 9 km LST/NDVI is not readily available. To remedy this lack of coarse data, 1 km LST/NDVI was upscaled to that of 9 km. The 1 km rasters of LST and NDVI data are available from AppEEARS in Sinusoidal, Lambert, and Geographic projections. It was observed that rasters using the Geographic projection aligned well with that of the EASE2.0 grids. To conduct the upscaling process, the Geographic projection 1 km LST and

NDVI rasters were first retrieved. This was done by using AppEEARS in conjunction with the 9 km shapefiles representative of the L4\_SM EASE2.0 grids discussed previously. Effectively, AppEEARS retrieved 1 km rasters of data across the entire 9 km shapefiles for use in upscaling. ArcGIS was then used to average the 1 km rasters across each EASE2.0 grid. The output from this upscaling process was LST and NDVI data at a resolution of 9 km that could then be used to determine the coarse SEE.

### 4.4 Downscaling and Locally Calibrating L4 SM Data

The downscaled L4\_SM is estimated using the difference between the fine SEE and the coarse SEE. This difference is then multiplied by the relationship between SM and SEE before adding the coarse scale L4\_SM. The downscaling routine is as follows:

$$SM_{1km} = SM_{L4\_SM} + \frac{\partial SM}{\partial SEE} (SEE_{1km} - SEE_{9km}) \tag{1}$$

where  $SM_{1km} =$  downscaled L4\_SM;  $SM_{L4\_SM} = 9$  km L4\_SM;  $\partial SM/\partial SEE =$  the approximation of the relationship between SM and SEE;  $SEE_{1km} =$  fine resolution SEE from 1 km LST/NDVI; and  $SEE_{9km} =$  coarse resolution SEE from upscaled LST/NDVI.

$$SEE = \frac{T_{S,max} - T_S}{T_{S,max} - T_{S,min}} \tag{2}$$

$$T_{s} = \frac{T_{LST} - 0.5 \cdot f_{v}(T_{v,min} + T_{v,max})}{1 - f_{v}}$$
 (3)

$$f_v = \frac{NDVI - NDVI_S}{NDVI_v - NDVI_S} \tag{4}$$

$$T_{v,max} = \max\left(\frac{T_{LST} - T_{s,max}(1 - f_v)}{f_v}\right)$$
 (5)

where SEE = either fine or coarse resolution SEE (depending on the resolution used);  $T_s$  = soil skin temperature (K);  $T_{s,min}$  = minimum of LST (K);  $T_{s,max}$  = maximum of LST (K);  $T_{v,min}$  = minimum of LST (K);  $T_{LST}$  = daily LST;  $f_v$  = fractional vegetation cover; NDVI = daily NDVI;  $NDVI_s$  = soil cover fraction (user observed); and  $NDVI_v$  = vegetation cover fraction (user observed).

An important part of the downscaling algorithm is the estimation of the relationship between SM and SEE (Colliander et al., 2017). This estimation is as follows:

$$\frac{\partial SM}{\partial SEE} = \alpha \cdot \frac{1}{N} \sum_{i=1}^{N} \frac{SM_{L4\_SM,i}}{SEE_{9km,i}} \tag{6}$$

where  $\alpha$  = experimental tuning parameter (observed to range between -1 and 1); and N = number of days.

The L4\_SM data was not only downscaled from 9 km to 1 km but was also locally calibrated to that of ground-based data. The calibration method used during this study was the application of simple multiplicative and additive offset factors to that of the downscaled data. The application of these offset factors to the downscaled data is follows:

$$SM_{cal} = (SM_{1km} \cdot MF) + AF \tag{7}$$

where  $SM_{cal}$  = site specific calibrated SMAP L4\_SM data;  $SM_{1km}$  = downscaled SM\_L4 data; MF = multiplicative factor (ranging from 0.0 - 1.0); and AF = additive factor (ranging from -1.0 - 1.0).

The calibration and downscaling routines were conducted in unison during this study. It was observed that the possible variability in the determination of the  $\alpha$ ,  $NDVI_s$ , and  $NDVI_v$  terms could lead to varying success during the downscaling routine when the downscaled data was compared to ground-based data. To conduct both routines in unison, a least squares optimization was conducted using the Microsoft Excel GRG nonlinear solver. This routine was carried out by the user first determining a range of  $\alpha$ ,  $NDVI_s$ , and  $NDVI_v$  that yielded downscaled data that compared well with the ground-based data. These ranges, as well as the ranges for the MF and AF discussed previously, were then used with the GRG nonlinear solver. The optimized downscaled and calibrated data was observed to follow the trend of the ground-based data better than that of the data obtained by the user generated ranges. Table 4 shows the optimized values for downscaling data at the ground-based sites.

Table 4. Optimized Downscaling and Calibration Values

Station	α	$NDVI_s$	$NDVI_v$	MF	AF	$\mathbb{R}^2$
Cook						
Farm	-0.0061	0.0139	0.832	1.0	0.168	0.912
Field						
Lind #1	-0.0004	0.0092	0.95	0.398	-0.002	0.753
Santa	1.0	0.092	0.881	0.153	0.462	0.459
Barbara	1.0	0.092	0.881	0.133	0.402	0.439
Yosemite	0.261	0.051	0.758	0.770	-0.058	0.969

The local calibration and downscaling efforts can be seen in the following figures (Figures 2-5). Figures 2A-5A represent the 9 km L4\_SM data taken over the calibration sites compared to that of the ground-based data taken from the in-situ sensor stations. Figures 2B-5B represent the calibration and downscaling efforts at each ground-based site. It is important to note that the plots labeled "RAW OS L4\_SM" represent 9 km data solely calibrated using the multiplicative and additive offsets discussed in Equation 7. No downscaling efforts were conducted on data within these plots. Alternatively, "DS & OS L4\_SM" plots represent downscaled (1 km) and locally calibrated L4 SM data.

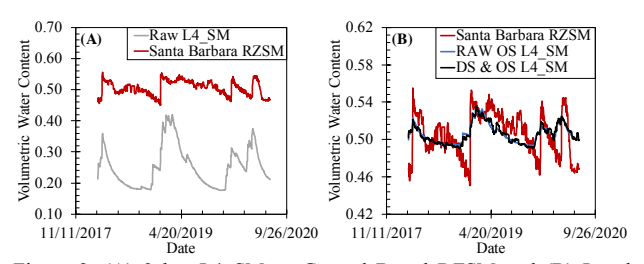


Figure 2. (A) 9 km L4\_SM vs Ground Based RZSM and (B) Local Calibration using Downscaled (1 km) and Raw (9 km) L4\_SM at the Santa Barbara USCRN Site

The downscaled calibrated data was observed to perform marginally better in Figures 2B and 3B. For example, this can be observed in Figure 3B within the boxed region on the plot where the downscaled data is seen to better reflect the drying trend observed within the in-situ data. However, in Figures 4B and 5B the downscaled calibrated data was seen to perform significantly better than that of the calibrated raw data. In general, the downscaled and locally calibrated L4\_SM data was observed to represent the in-situ data from all ground-based sites well.

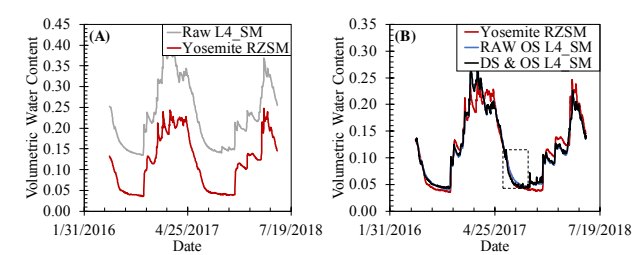


Figure 3. (A) 9 km L4\_SM vs Ground Based RZSM and (B) Local Calibration using Downscaled (1 km) and Raw (9 km) L4\_SM at the Yosemite USCRN Site

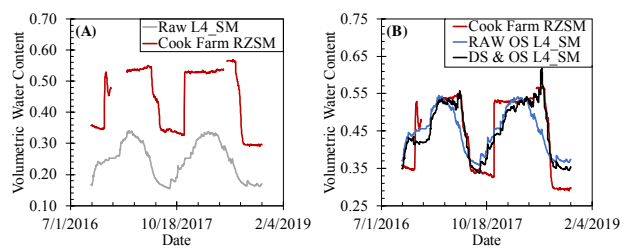


Figure 4. (A) 9 km L4\_SM vs Ground Based RZSM and (B) Local Calibration using Downscaled (1 km) and Raw (9 km) L4\_SM at the Cook Farm Field SCAN Site

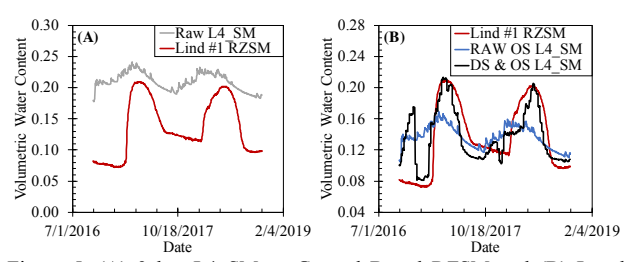


Figure 5. (A) 9 km L4\_SM vs Ground Based RZSM and (B) Local Calibration using Downscaled (1 km) and Raw (9 km) L4\_SM at the Lind #1 SCAN Site

For downscaling at the landslide sites, the averages of the data shown in Table 4 were applied to the corresponding landslide site. It is worth noting that the average of the tuning parameter  $(\alpha)$  returned poor results at the Mud Creek site and was replaced by a user chosen value. This implies that the tuning parameter may be a purely site-specific variable. Table 5 shows the values applied to the landslide sites as well as what network was used in the calibration process. It also must be again noted that Sierra Leone has no optimized values due to the lack of ground-based data. In the subsequent stability analysis discussions, raw L4\_SM data was investigated at the Sierra Leone site.

Table 5. Optimized Downscaling and Calibration Values at Landslide Sites

Sites						
Landslide	Network	α	$NDVI_s$	$NDVI_v$	MF	AF
Mud Creek	USCRN	0.01	0.072	0.819	0.461	0.202
Rattlesnake	SCAN	-0.003	0.012	0.891	0.699	0.083
Sierra Leone	N/A	N/A	N/A	N/A	N/A	N/A

It is understood that biases may be being introduced to the downscaled data due to being directly calibrated to ground-based data at individual locations. This possibility is why calibrations and downscaling variables are averaged over the calibration sites before being applied to their respective landslide sites. Future studies using the local calibration and downscaling routines will

make use of more local calibration sites to minimize potential site biases.

### 5 GEOTECHNICAL AND LAND SURFACE DATA

Due to the catastrophic failures of the Mud Creek and Sierra Leone landslides, and the threat posed by the Rattlesnake Hills creeping slide, many researchers (Machan et al., 2018; Norrish, 2018) have conducted studies into the physical and geotechnical properties of said slides. Investigated geotechnical properties include slope angle, depth to slip surface, friction angle, and cohesion,  $\beta$ ,  $H_{ss}$ ,  $\phi'$ , and c', respectively. In the case of the Mud Creek and Rattlesnake Hills slides, the soil compositions (i.e., % sand, % silt, and % clay) were unavailable from published research. To account for this lack of data, borehole information from either the California Geological Survey (CGS) or the Washington Department of Natural Resources (DNR) was utilized. The geotechnical and land surface data acquired from either published work, or the borehole information, is shown in Tables 6 and 7. Additionally, Table 7 presents the saturated and residual volumetric water content data,  $\theta_s$  and  $\theta_r$ , respectively. These data are assumed to be representative of in-situ conditions at the onset of the investigated landslides. The saturated water content was obtained through analysis of the downscaled SMAP L4 SM data. The maximum volumetric water content value at each site over a two-year period (one-year prior to and one-year after the event) were assumed to be indicative of the saturated values.

Table 6. Geotechnical Data for Three Investigated Landslide Events

Landslide	β	$H_{ss}$	$\phi'$	c'
Lanusine	(deg)	(m)	(deg)	(kPa)
Mud Creek	36.5	35	34.5	0
Rattlesnake	14.5	30	14	0
Sierra	35	7.5	18	28
Leone	33	7.5	10	20

Table 7. Land Surface Data for Three Investigated Landslide Events

Landslide	% Sand	% Clay	% Silt	$\theta_s$ (cm <sup>3</sup> /cm <sup>3</sup> )	$\theta_r$ (cm <sup>3</sup> /cm <sup>3</sup> )
	Bana	City	Diff	(cm /cm )	(cm /cm )
Mud Creek	65.2	17.4	17.4	0.410	0.0527
Rattlesnake	96.5	1.75	1.75	0.273	0.0483
Sierra Leone	67	19	14	0.413	0.0564

For the Sierra Leone landslide: (1) 9 km SMAP L4\_SM (i.e., non-downscaled) data was used in the analysis due to lack of ground-based data. (2) Data such as  $\phi'$  and c' were not available at the site of the slide. However, Igwe (2018) conducted research on a nearby landslide in Nigeria. Due to the lack of borehole information and/or research data from the physical site, data from Igwe (2018) was substituted where needed.

### 6 HYDROLOGIC BEHAVIOR VIA DOWNSCALED SMAP L4 SM

For the associated stability analyses using the previously discussed locally calibrated downscaled SMAP L4\_SM data, the Lu and Godt (2008) infinite slope stability equation was used. A more encompassing discussion of this equation and its results will follow in Section 7. However, a key variable for this equation is that of suction stress. Suction stress is given as:

$$\sigma^s = S_e s \tag{8}$$

where  $\sigma^s$  = suction stress (kPa);  $S_e$  = effective degree of saturation =  $(\theta - \theta_r)/(\theta_s - \theta_r)$ ;  $\theta$  = volumetric water

content;  $\theta_r$  = residual volumetric water content;  $\theta_s$  = saturated volumetric water content; and s = matric suction =  $(u_a - u_w)$ ;  $u_a$  = pore air pressure;  $u_w$  = pore water pressure. The effective degree of saturation is a variable that can be

The effective degree of saturation is a variable that can be calculated via SMAP L4\_SM data. However, data for matric suction, a function of the hydrologic behavior of the soil (i.e., the change in water content or degree of saturation due to suction), was not readily available at the landslide study sites. To remedy this lack of data, the soil water characteristic curve (SWCC) model established by van Genuchten was manipulated to yield matric suction and adopted for this study. The manipulated van Genuchten SWCC equation is given as:

$$s = \frac{1}{\alpha} \left[ \left( \frac{1}{S_e} \right)^{1/m} - 1 \right]^{1/n} \tag{9}$$

where s = matric suction;  $S_e =$  effective degree of saturation;  $\alpha$ , n and m = fitting parameters reflecting the air entry value, the slope at the inflection point of the SWCC, and the curvature of the SWCC near the residual point, respectively.

With the adoption and manipulation of the SWCC curve to output an equation yielding matric suction comes the requirement of the determination of the fitting parameters  $\alpha$ , n and m. To obtain these fitting parameters, pedotransfer functions (PTFs) included in the Rosetta Lite software, embedded in the HYDRUS flow simulation software were used. The inputs for the PTFs are the % sand, % silt, % clay data presented in Table 7. The Rosetta output includes estimates of  $\theta_r$ ,  $\theta_s$  (however, the saturated value presented in Table 7 was used in the calculations),  $\alpha$ , and n. The Rosetta PTFs use the approximation that states m=1-1/n. The van Genuchten fitting parameters used in this study are shown in Table 8.

Table 8. Land Surface Data for Three Investigated Landslide Events

Landslide	α	n	m
Mud Creek	0.028	1.373	0.2715
Rattlesnake	0.0304	3.355	0.702
Sierra Leone	0.027	1.371	0.271

## 7 LANDSLIDE SLOPE STABILITY ANALYSIS WITH DOWNSCALED L4 SM DATA

For this study, the known landslide locations were analyzed using an infinite slope stability equation derived by Lu and Godt (2008). The general form of the Lu and Godt (2008) infinite slope equation is as follows:

$$FS = \frac{\tan(\phi')}{\tan(\beta)} + \frac{2c'}{\gamma H_{SS} \sin(2\beta)} + r_u [\tan(\beta) + \cot(\beta)] \tan(\phi')$$
(10)

where FS = factor of safety;  $\phi'$  = soil friction angle; c' = effective soil cohesion;  $\beta$  = slope angle;  $\gamma$  = soil unit weight (assumed to be  $17.28 \ kN/m^3$ );  $H_{SS}$  = depth to bedrock (meters);  $r_u$  = pore pressure ratio =  $\sigma^S/\gamma H_{SS}$ ; and  $\sigma^S$  = suction stress.

The soil shear strength and slope parameters used for the calculation of the FS throughout this study are given in Table 6. The Mud Creek and Rattlesnake Hills landslides had no relevant cohesion (c') data and were therefore assumed to be purely frictional (i.e., c' = 0 kPa) due to their composition being assumed predominantly sandy due to borehole data.

The intention behind using downscaled satellite-based soil moisture (i.e., L4\_SM) in slope stability analyses was to investigate the feasibility of remotely and accurately detecting incipient landslide conditions. As discussed, this study made use of downscaled and calibrated L4 SM at two landslide sites, and

raw L4\_SM at a third. Figure 6 shows plots of calculated FOS using both downscaled and raw L4\_SM at the Mud Creek and Rattlesnake Hills landslide sites. As seen in Figure 6A, the raw FOS (from 9 km L4\_SM) is seen to be increasing at the time of failure. This implies that the soil in the slope was strengthening, rather than weakening, at failure. However, the downscaled FOS (from 1 km L4\_SM) is seen to be at 1.0 at the time of failure, with an immediate strengthening of the soil shown after failure (i.e., by the FOS increasing after failure). Therefore, in the case of the Mud Creek site, the downscaled FOS functioned better in detecting incipient conditions than that of the raw FOS.

However, this same trend is not observed when comparing raw and downscaled FOS at the Rattlesnake Hills site. As seen in Figure 6B, both raw and downscaled FOS follow the same trend of decreasing after the time referred to as failure (assumed to be 10/20/2017 in this study). Although both datasets follow the trend of decreasing, it is the raw FOS that reaches a FOS of 1.0 shortly after failure was reported. It is necessary to note that failure at the Rattlesnake site was not a catastrophic failure. The failure is instead a slow-moving failure that creeps at a constant velocity of two to three inches per day (Norrish, 2018). Additionally, surface fissures were reported by a pilot flying over the site near the time referred to as "failure" in this study. These fissures indicate the soil was moving. Therefore, incipient conditions were not reflected by either FOS at the time referred to as failure, but a weakening of the soil was occurring. This weakening was reflected by both raw and downscaled FOS datasets remaining near a FOS = 1.0, which is promising for the goal of detecting incipient conditions remotely.

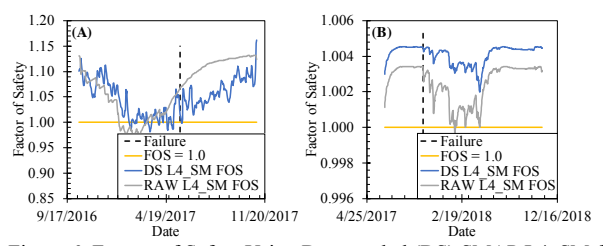


Figure 6. Factors of Safety Using Downscaled (DS) SMAP L4\_SM for: (A) Mud Creek Landslide and (B) Rattlesnake Hills Creeping Landslide

Figure 7 shows the raw FOS at the Sierra Leone landslide site. As discussed, no ground-based data was available for this site, so no downscaling was able to be conducted.

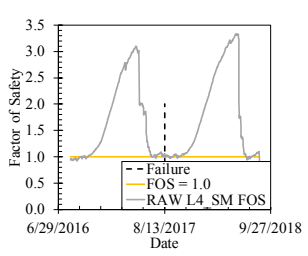


Figure 7. Factor of Safety Using Raw SMAP L4\_SM for Sierra Leone Landslide

However, as can be seen in Figure 7, the raw FOS does indicate incipient conditions at the time of failure (i.e., FOS = 1.0). It can also be seen that the FOS reached 1.0 approximately one month before the time of failure. This can likely be explained by the fact that Sierra Leone received approximately three times the usual amount of rainfall in the weeks leading up to the failure. However, why the landslide did not occur as soon as the FOS reached 1.0 (i.e., incipient conditions), is not clear. Further research is required to; (i) Better understand the hydrologic mechanisms at work during landslide occurrence to better answer this question and (ii) Determine if downscaling of L4\_SM data is required for use in accurate landslide FOS analyses.

#### 8 CONCLUSIONS

The goal behind this study was: First, to show the feasibility of downscaling and calibrating SMAP Rootzone Soil Moisture (L4\_SM) to that of ground-based data. Second, to downscale and use L4 SM data at known landslide locations to determine if incipient conditions at failure can be detected by remotely sensed data (i.e., satellite-based soil moisture). From this study, it can be noted that downscaled L4\_SM data can be both retrieved and used in slope stability analyses to detect incipient failure and/or strength weakening conditions at the analyzed landslide sites. This can be observed at the Mud Creek (incipient) and Rattlesnake (strength weakening) sites. However, it was also observed that raw (i.e., non-downscaled) L4 SM data functioned well in detecting these same conditions. The raw L4\_SM was observed to detect strength weakening at Rattlesnake and incipient conditions at Sierra Leone. Additionally, further research is required to ascertain a better understanding of hydrologic mechanisms at work during landslide occurrence. This future research is expected to yield a better understanding as to why failure does not occur as soon as the FOS reaches 1.0 (e.g., as seen at Mud Creek and Sierra Leone). In general, it is thought that this current study has laid a framework upon which higher resolution remotely sensed SM (1 km or finer in future studies) can be retrieved via downscaling and then utilized for the application of landslide slope stability analysis.

#### 9 REFERENCES

Brodzik, M. J., Billingsley, B., Haran, T., Raup, B., and Savoie, M. H. (2012). "EASE-Grid 2.0: Incremental but Significant Improvements for Earth-Gridded Data Sets." *ISPRS International Journal of Geo-Information*, MDPI AG, 1(1), 32–45.

Chan, S. K., Bindlish, R., O'Neill, P. E., Njoku, E., Jackson, T., Colliander, A., Chen, F., Burgin, M. S., Dunbar, S., Piepmeier, J. R., Yueh, S., Entekhabi, D., Cosh, M. H., Caldwell, T. G., Walker, J. P., Wu, X., Berg, A., Rowlandson, T., Pacheco, A., McNairn, H., Thibeault, M., Martínez-Fernández, J., González-Zamora, Á., Seyfried, M., Bosch, D. D., Starks, P., Goodrich, D., Prueger, J., Palecki, M. A., Small, E. E., Zreda, M., Calvet, J.-C., Crow, W., and Kerr, Y. (2016). "Assessment of the SMAP Passive Soil Moisture Product." *IEEE Transactions on Geoscience and Remote Sensing*, 54(8), 1–14.

Colliander, A., Fisher, J. B., Halverson, G., Merlin, O., Misra, S., Bindlish, R., Jackson, T. J., and Yueh, S. (2017). "Spatial Downscaling of SMAP Soil Moisture Using MODIS Land Surface Temperature and NDVI During SMAPVEX15." *IEEE Geoscience and Remote Sensing Letters*, 14(11), 2107–2111.

Hong, Y., Adler, R., and Huffman, G. (2007). "Use of satellite remote sensing data in the mapping of global landslide susceptibility." *Natural Hazards*, 43(2), 245–256.

Igwe, O. (2018). "The characteristics and mechanisms of the recent catastrophic landslides in Africa under IPL and WCoE projects." *Landslides*, 15, 2509–2519.

Lu, N., and Godt, J. (2008). "Infinite slope stability under steady unsaturated seepage conditions." Water Resources Research, 44(11).

Norrish, N.I. (Wyllie & Norrish Rock Engineers, Inc.), I-82, MP 36 to 44, Rattlesnake Hills Landslide Evaluation, Report prepared for Washington Department of Transportation and Department of Natural Resources (Washington Geological Survey), January 30, 2018.

Machan, G., Hammond, C., and Westover, T. (2018). "Rattlesnake Hills Landslide: Overview and Monitoring." 69th Highway Geology Symposium, Portland, Maine, 10 – 13 September 2018.

Merlin, O., Walker, J. P., Chehbouni, A., and Kerr, Y. (2008). "Towards deterministic downscaling of SMOS soil moisture using MODIS derived soil evaporative efficiency." Remote Sensing of Environment, 112(10), 3935–3946.

Terzis, A., Anandarajah, A., Moore, K., and Wang, I.-J. (2006). "Slip surface localization in wireless sensor networks for landslide prediction." 2006 5th International Conference on Information Processing in Sensor Networks.